Chemistry–A European Journal

Communication
doi.org/10.1002/chem.202101246

Chemistry
Europe
European Chemical
Societies Publishing

TIPS-Ethynylated Naphthodiquinoline and Naphthodiacridine: Novel Diazabisacenes

Lukas Ahrens,[a] Steffen Maier,[a] Erik Misselwitz,[a] Thomas Oeser,[a] Frank Rominger,[a] Jan Freudenberg,*[a] and Uwe H. F. Bunz*[a, b]

Abstract: The synthesis of two diazabisacenes is reported. A bisboronated naphthalene was Suzuki-coupled to substituted ethyl nicotinates, then cyclized by intramolecular Friedel-Crafts acylation. The resulting diketones were alkynylated and reduced to give the title compounds, bis(TIPS-ethynyl)-substituted naphtha[1,8-*gh*:5,4-*g'h'*]diquinoline and naphtho[1,8-*bc*:5,4-*b'c'*]diacridine. Nitrogen incorporation stabilizes the bisacenes with respect to oxidation compared to their consanguine nonaza analogs.

Linear annellation of benzene rings gives members of the acene family[1] – a structural class indispensable for organic electronics. Applications range from organic field effect transistors[2] to memory devices[3] or third-generation organic photovoltaics relying on singlet fission.[4] The longer acenes are limited by their sensitivity towards oxygen.[5] To meet this issue, acenes were stabilized[6] by silylethynylation,[7,8] encapsulation[9] or benzannulation[10] – the latter capitalizing on an increased number of Clar sextets. Extending this approach, the connection of two acenes by sharing at least one common bond on the zigzag edge (highlighted in red in Figure 1) leads to bisacenes[11,12] such as **A**, **B** of increased stability[13,14] and p-type mobilities of up to 6.1 cm² V⁻¹ s⁻¹ for single crystal transistors of **B**.[11,15] Introduction of nitrogen into the backbone of acenes tunes optoelectronics and increases stability towards oxidation.[16–19] Azaacenes are attractive n-type semiconductors
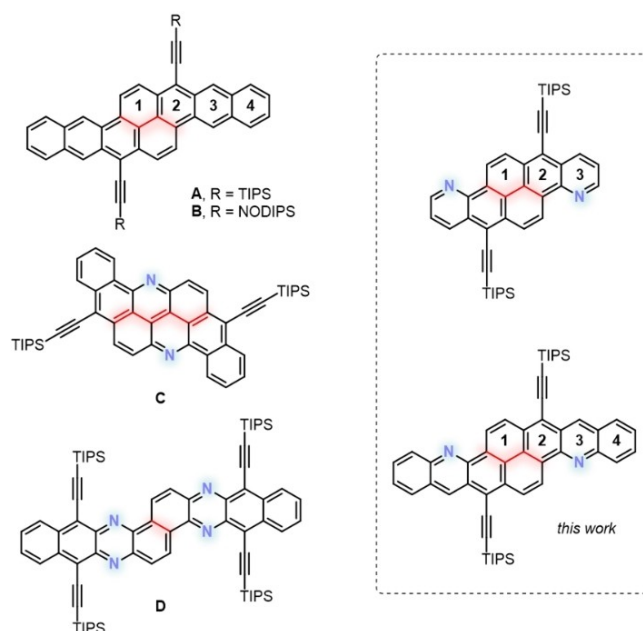

Figure 1. Selected examples of (aza)bisacenes (left) and structures investigated here (right) along with the ring numbering applied throughout this work.[11,20,21] The zigzag edge connecting the two formal (aza)acene subunits is highlighted in red. TIPS = tri*iso*propylsilyl; NODIPS = *n*-octyld*iso*propylsilyl.

but nitrogen substitution is less known for heteroatom doped bisacenes (cf. **C**, **D**).[20,21]

For the synthesis of the azabisacenes of type **A**, we used the route of Briseno et al.[11] Starting from 1,5-bisborylated naphthalene **1**, Suzuki coupling with the bromides **2 a,b** gave esters **3 a,b**. After saponification the carboxylic acids **4 a,b** were obtained in excellent yields (Scheme 1, top). The polyphosphoric acid (PPA) promoted ring closure furnished quinones **5 a,b** in 60–70% yield. The addition of TIPS-ethynyl lithium or the corresponding Grignard reagent was followed by reduction with SnCl₂, the bottleneck of the synthesis as it gave **6 a** in 5% yield and **6 b** in 21% yield after optimization.

The targets are formed selectively, yet in small yields. Attempts to synthesize the tetraaza analog of **A** failed (see the Supporting Information) as the pyrazinic precursor of type **4** decarboxylates upon attempted ring closure. The nicotinates **4 a,b** were thermally stable and unaffected by this issue.
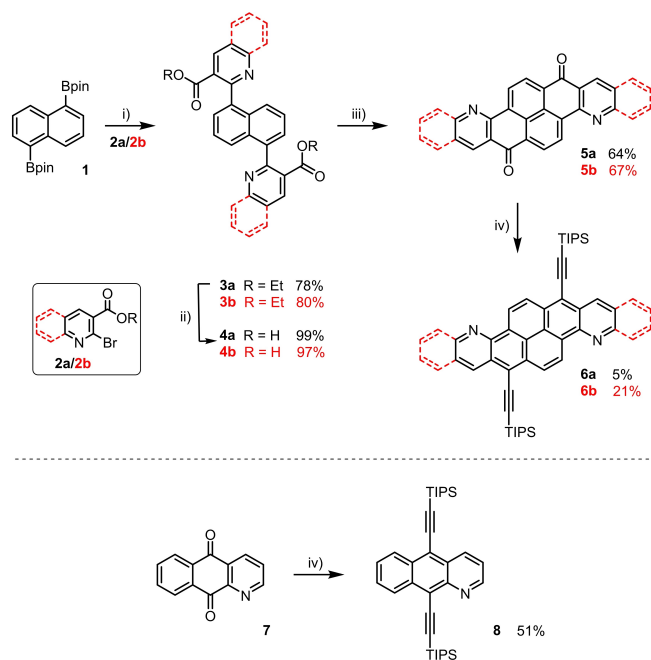
Azaanthracene **8**, a formal subunit of bisanthracene **6 a**, was synthesized for comparison. Starting from the literature known quinone **7**[22] using a standard alkynylation procedure, **8** was obtained in 51% yield (Scheme 1, bottom).

[a] L. Ahrens, S. Maier, E. Misselwitz, Dr. T. Oeser, Dr. F. Rominger, Dr. J. Freudenberg, Prof. Dr. U. H. F. Bunz
Organisch-Chemisches Institut
Ruprecht-Karls-Universität Heidelberg
Im Neuenheimer Feld 270, 69120 Heidelberg (Germany)
E-mail: freudenberg@oci.uni-heidelberg.de
uwe.bunz@uni-heidelberg.de

[b] Prof. Dr. U. H. F. Bunz
Centre for Advanced Materials (CAM)
Ruprecht-Karls-Universität Heidelberg
Im Neuenheimer Feld 225, 69120 Heidelberg (Germany)

Chemistry–A European Journal

Communication
doi.org/10.1002/chem.202101246

Chemistry Europe
European Chemical
Societies Publishing

Scheme 1. Synthesis of diazabisacenes **6a,b** and model compound **8**. i) **2a** or **2b**, K_2CO_3, Pd(PPh$_3$)$_4$, THF, H_2O, 80 °C, 3 d; ii) KOH, THF, MeOH, 80 °C, 4 h; iii) PPA, 140–170 °C, 16 h–3 d; iv) 1) iPr$_3$SiCCH, n-BuLi, THF, −78 °C→RT, 16 h; 2) SnCl$_2$, HCl, THF, RT, 3 h.

The diazabisacenes **6a**, **6b** and azaanthracene **8** are isolated as orange, blue and yellow crystalline solids, respectively. Figure 2 displays the absorption and emission spectra of **6a,b** and **8** in n-hexane and a photograph of the solutions of **6a,b** under daylight and UV light (365 nm). When comparing the absorption spectrum of **6a** to that of azaanthracene **8**, a red-shift of 66 nm (2927 cm^{-1}) is observed – testament to the enlarged π-system and electronic coupling between formal
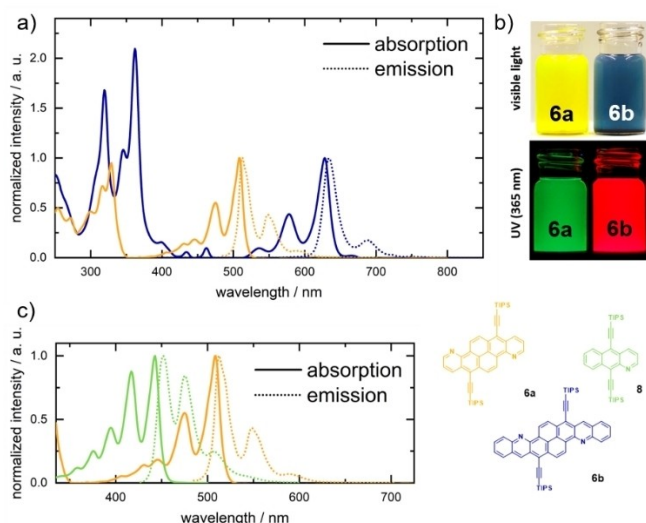
azaacene subunits. When going from **6a** to **6b**, we see a red-shift of 119 nm (3723 cm^{-1}). Similar to the linear acenes, the absorption spectra of the azabisacenes display well-resolved "acene fingers" (p-bands) with the most dominant contribution involving the two vibrational ground states of $S_0{\rightarrow}S_1$, attributable to a HOMO-LUMO transition as evidenced by quantum-chemical TD-DFT calculations (see Section S7 in the Supporting Information).[23,24] This is in accordance with the findings of Briseno et al. for **A**.[11] All three compounds are visibly emissive in dilute n-hexane solution following the mirror image rule. Quantum yields are 87, 77 and 35% for **8**, **6a** and **6b**, decreasing with smaller optical gaps (Table 1). The Stokes shifts of approximately 150 cm^{-1} for both **6a,b** are smaller than that for azaanthracene **8** (450 cm^{-1}). Nitrogen incorporation preserves spectral shape but slightly blue-shifts the absorption and emission maxima in comparison to those of **A** ($\lambda_{max,abs} =$ 635 nm).

Optical spectra allow for an easy assessment of the stability of **6a,b** and **8** in solution. To monitor their persistence under ambient conditions in solution (10^{-5} M), the time-dependent decrease of absorption at λ_{max} was recorded in toluene and in chloroform (see the Supporting Information). Briseno et al. observed a 20% decrease of absorption of **A** in chloroform after 1 d[11] – a similar drop in intensity for its aza-congener **6b** took 14 d. Both **6a** and **6b** retained their absorption in toluene over 14 d – the same was observed for dilute solutions of **6b** in chloroform. Azaanthracene **8** is less persistent than **6a**. This can be explained in terms of oxidation activation barriers and distortion energies as was previously demonstrated for pentacene and bistetracene.[14]

The increased stability compared to **A** is expected; O_2 adduct formation was reported to preferably occur on ring 3 (cf. Figure 1) of bistetracene **A**,[14b] which is not possible in case of **6b** as the positions are occupied by nitrogen. To evaluate the redox potentials of the azabisacenes **6a** and **b**, cyclic voltammetry and DFT calculations were performed. Table 2 displays the electrochemical data, calculated ionization potentials and electron affinities of **6a**, **6b**, **8** and **A**. Bisanthracene **6a** is both easier reduced and oxidized electrochemically than its formal monomer **8** – in agreement with quantum-chemical DFT calculations, which also reproduce optical gaps fairly well.[23] HOMO and LUMO of nitrogen-substituted **6b** are stabilized by approximately 0.2 eV with respect to **A** contributing to **6b**'s oxidation resistance.

Single crystals of **6a,b** and **8** were obtained by slow diffusion of methanol into a chloroform solution of the

Figure 2. a) Normalized absorption and emission spectra of **6a** and **6b** in n-hexane. b) Photographs of **6a** and **6b** under daylight (top) and UV light (bottom, $\lambda_{ex} = 365$ nm) in n-hexane. c) Normalized absorption and emission spectra of **6a** and monoazaanthracene **8** in n-hexane.

Table 1. Optical properties of **6a**, **6b**, **8** and **A** in n-hexane.

Compd	$\lambda_{max, abs}$ [nm]	$\lambda_{onset, abs}$ [nm]	$\lambda_{max, em}$ [nm]	Stokes shift [cm^{-1}]	Φ	τ [ns]
6a	509	520	513	153	0.77	3.96
8	443	455	452	450	0.87	5.68
6b	628	644	634	151	0.35	4.63
A	635[a]	656[a]	_[b]	_[b]	_[b]	_[b]

[a] Data for **A** from ref. [11] measured in chloroform. [b] Emission spectrum, Φ and τ were not supplied in ref. [11].

Chemistry–A European Journal

Communication

doi.org/10.1002/chem.202101246

Chemistry Europe
European Chemical
Societies Publishing

Table 2. Experimental and calculated (gas-phase) properties of **6a**, **6b**, **8** and **A** in dichloromethane.

Compd	$E^{(0/-)}$ [V][a]	IP/HOMO [eV] meas.[b]/calcd[c]	EA/LUMO [eV] meas.[d]/calcd[c]	Gap [eV] meas.[e]/ calcd[c]
6a	−1.59	−5.89/−5.34	−3.51/−2.88	2.38/2.46
8	−1.78	−6.04/−5.61	−3.32/−2.70	2.72/2.91
6b	−1.30	−5.73/−5.11	−3.80/−3.17	1.93/1.94
A[f]	−1.40	−5.59/−4.91	−3.70/−2.99	1.89/1.92

[a] First reduction potentials from cyclic voltammetry (CV) in dichloromethane at room temperature with Bu_4NPF_6 as the electrolyte against Fc/Fc$^+$ as an internal standard (−5.10 eV) at 0.2 Vs^{-1}.[25] [b] $IP_{meas} = EA_{meas}$-gap_{meas}. [c] Obtained from DFT calculations (Gaussian 16: geometry optimization: B3LYP/def2-SVP// B3LYP/def2-TZVP; FMO calculations: B3LYP/def2-TZVP; TMS groups were used instead of TIPS).[23] [d] $EA_{meas} = -e(5.1 V + E^{(0/-)})$. [e] gap_{meas} calculated from λ_{onset} in n-hexane. [f] experimental data for **A** taken from ref. [11], CV measured in chlorobenzene at 0.1 Vs^{-1}.
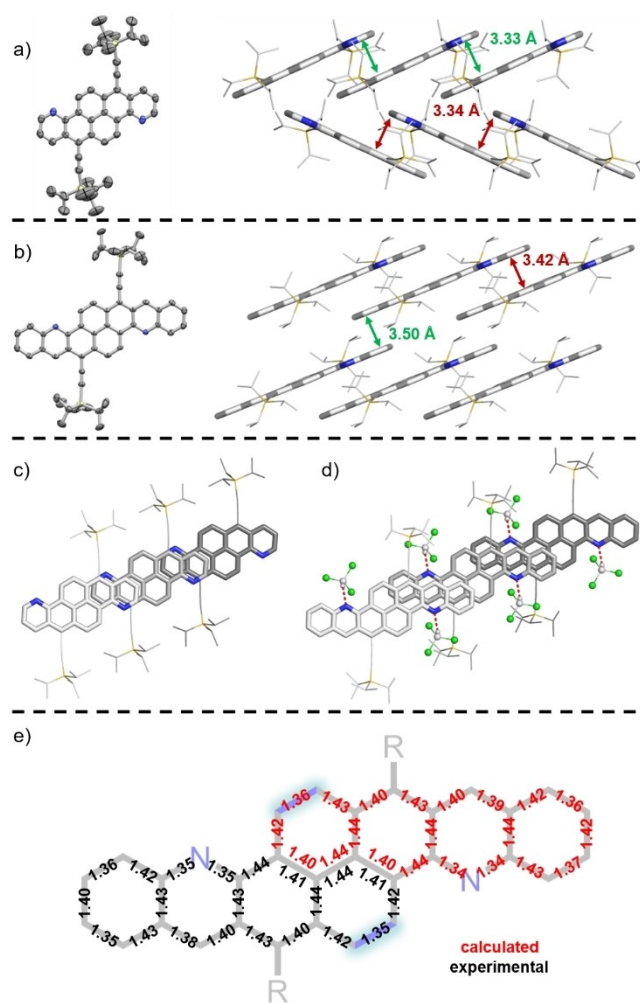

Figure 3. Solid-state structures (ellipsoids set to the 50% probability level) and visualization of packing of a), c) **6a** and b), d) **6b**. Co-crystallized chloroform is omitted for clarity in (b). e) Experimental and calculated bond lengths of **6b** (Gaussian 16: geometry optimization: B3LYP/def2-SVP// B3LYP/def2-TZVP[23]).

respective compound – the growth of suitable crystals of **6b** was difficult due to its poor solubility and tendency to precipitate as microcrystals. Monoazaanthracene **8** crystallizes in the orthorhombic space group *Pbca* with 8 molecules per unit cell (see Figure S41 in the Supporting Information for visualization of structure and packing). Van-der-Waals contacts between the acene core and the silyl groups of two neighboring molecules dominate molecular packing, resulting in edge-to-face orientation of adjacent π-systems and inhibiting π-stacking. The crystal structure is isomorphous to that of the TIPS-ethynylated anthracene (CCDC: 962668) sharing both space group and a similar unit cell[26] – the nitrogen atom of **8** is distributed statistically among the four possible atom positions and thus bond lengths can only represent mean values (see the Supporting Information). The extension of the arene backbone to bisacenes changes the packing in the solid state. Instead of an edge-to-face arrangement we observe π-stacking (face-to-face interactions) in both **6a** and **b** as the dominating packing feature. Bisanthracene **6a** crystallizes in the monoclinic space group $P2_1/c$ (2 per unit cell). Its chromophores adopt a slipped herringbone arrangement with π-stacking distances of 3.33–3.34 Å between the molecules within the stacks.

The overlap of the aromatic core involves two benzene rings on each side of the aromatic backbone within the stack (rings 2 and 3, Figure 3c) – adjacent stacks show no π-interactions (Figure 3a).

Bistetracene **6b** crystallizes as solvate with chloroform, whose proton interacts with the pyridinic nitrogens, (close contact C···N = 3.30 Å, see Figure 3d and the Supporting Information) in the triclinic space group $P\bar{1}$. Benzannulation of two additional rings in bistetracene **6b** increases the overlap between stacked molecules; π-stacking distances of 3.42 Å result within the 1D slipped-stack arrangement. Additional π-stacking is observed between neighboring stacks (3.50 Å, ring 4) and is not diminished by the intercalated chloroform molecules. The hydrocarbon **A** (CCDC: 1427378) also crystallizes in a 1D slipped-stack (3.41 Å) sharing the same space group $P\bar{1}$ and number of molecules in the unit cell, but without solvent

intercalation and, more importantly, without overlap of adjacent stacks.[11] This is noticeable as in most but not all cases the N-arenes crystallize similarly to their hydrocarbon counterparts.

While the bathochromic shifts in the absorption spectra indicate the electronic interaction of the formal acene-subunits in bisacenes **6a,b**, bond lengths, NMR shifts and theoretical methods help to evaluate the conjugation and aromaticity of these arenes. The core fragment of these bisacenes is structurally similar to pyrene. For instance, the bonds in rings 2 for **6a** and **6b** show only little length variation (exp. 1.40–1.43 Å for **6a**, 1.40–1.44 Å for **6b**) – a sign of delocalization within these rings. Noticeable, however, are the increased bonds lengths on the armchair edge (highlighted in blue in Figure 3e) of the "π-extended pyrenes" **6a** (1.35 Å, see the Supporting Information) and **6b** (1.34 Å) compared to pyrene itself (exp. 1.32 Å, CCDC: 1240734).[27] In the latter, the π-electrons appear to be more localized whereas in the bisacenes they are of similar lengths as those found on the outer *cata*-edges (ring 3 for **6a**,

Chemistry–A European Journal

Communication
doi.org/10.1002/chem.202101246

Chemistry
Europe
European Chemical
Societies Publishing

ring 4 for **6b**, respectively). Additionally, the central bond (shared between rings 1 and 1') is slightly elongated in the bisacenes (exp. 1.43 Å for **6a**, exp. 1.44 Å for **6b** vs. exp. 1.41 Å for pyrene).[27] This suggests that the resonance structure for **6a,b** depicted in Scheme 1 contributes to the electronic structure; however, not to the same extent as in the case of pyrene. Similar to acenes[28] bond length alternation is observed for the individual acene fragments in **6b** with the characteristic inversion of alternation of long and short bonds on the carbonaceous zigzag edge near the center (between rings 2 and 3) of the individual acene moieties. This observation is less pronounced for bisanthracene **6a**.

The perimeter of the bisacenes contains 22 and 30 π-electrons for bisanthracene **6a** and bistetracene **6b**, respectively, suggesting global Hückel aromaticity ($4n+2$, $n=5$ for **6a** and $n=7$ for **6b**). This is supported by low-field resonances in ^{1}H NMR for the protons on the respective backbones. To further investigate aromaticity in the bisacene motif, we calculated NICS(1) values for **6a,b** and **8** (Figure 4). All of the rings display negative shifts, that is, significant aromaticity. The central naphthalene unit of **6a,b** is the least aromatic segment, corroborating the bond length analysis. The anisotropy of the current induced density (AICD) plot[29] of **6b** (and **6a**, see the Supporting Information) is consistent with the NICS calculations; the clockwise diatropic ring current is mainly delocalized around the perimeter (red arrows in Figure 4, bottom) – the bisacenes exhibit global aromaticity with a little bypass of ring current (blue arrows) in the central pyrene rings (rings 1). These rings are – consistent with NICS calculations and the observed bond lengths – less aromatic (see the Supporting Information for the calculations for **6a** and **8**).

In conclusion, the first diazabistetracene **6b** and diazabisanthracene **6a** have been prepared and characterized. Nitrogen incorporation lowers the ionization potential and increases the electron affinity by around 0.1 eV per nitrogen atom and makes the bisacene more resistant towards degradation. Both compounds exhibit global aromaticity with bond length alternations and optical spectra similar to those of acenes, thus justifying the term "bisacenes" for the compounds investigated. To achieve a lower-lying LUMO, that is, higher electron affinity, more ring nitrogen atoms should be introduced into the skeleton. We are currently reinvestigating the synthesis of **6a** and varying the silyl substituents for **6b** to improve yields and solubility for the processing of thin films and the application of azabisacenes in thin-film transistors.

Experimental Section

Syntheses: **1**,[30] **2b**[31] **7**,[22] and **S1**[32] were synthesized according to literature procedures. Deposition numbers 2068043 (for **6a**), 2068044 (for **6b**) and 2071304 (for **8**) contain the supplementary crystallographic data for this paper. These data are provided free of charge by the joint Cambridge Crystallographic Data Centre and Fachinformationszentrum Karlsruhe Access Structures service.

General procedure for the preparation of N-bisacenes: In a heatgun dried Schlenk tube under an atmosphere of argon n-butyllithium (5.80 equiv., 2.50 mol L^{-1}) was added dropwise to a solution of tri*iso*propylsilylacetylene (6.00 equiv.) in anhydrous THF at −78 °C. The reaction mixture was allowed to warm to room temperature and stirred for 1 h. Quinone **5** (1.00 equiv.) was added, and the mixture was stirred at room temperature for 16 h. SnCl$_2$·2H$_2$O (4.00 equiv.) in aqueous HCl (6.50 equiv., 3.00 mol L^{-1}) was added and the solution was stirred at room temperature for 3 h. The reaction was quenched with water, neutralized with aqueous NaHCO$_3$ solution and extracted with dichloromethane. The combined organic layers were dried over magnesium sulfate and filtrated. The solvent was removed under reduced pressure and the crude product was absorbed on Celite. After flash column chromatography (petroleum ether/diethyl ether 500:1 v/v) the product **6** was isolated.

7,14-Bis{[tri*iso*propyl)silyl]ethynyl}naphtho[1,8-*gh*:5,4-*g′h′*] diquinoline (**6a**): orange solid; $R_f = 0.65$ (SiO$_2$; petroleum ether/ethyl acetate 5:1, v/v); M.p.: 296 °C; ^{1}H NMR (CDCl$_3$, 400 MHz, RT): $\delta = 9.75$ (d, $J = 9.4$ Hz, 2H), 9.28 (dd, $J = 4.1$ Hz, $J = 1.8$ Hz, 2H), 9.18 (dd, $J = 8.5$ Hz, $J = 1.8$ Hz, 2H), 9.06 (d, $J = 9.4$ Hz, 2H), 7.80 (dd, $J = 8.5$ Hz, $J = 4.0$ Hz, 2H), 1.29–1.44 ppm (m, 42H); ^{13}C{^{1}H} NMR (CDCl$_3$, 101 MHz, RT): $\delta = 150.1, 142.2, 135.4, 132.9, 129.5, 127.8, 127.3, 125.5, 125.0, 122.5, 116.7, 105.1, 103.2, 19.1, 11.7$ ppm; IR (ATR): $\tilde{\nu} = 2924, 2864, 1463, 1259, 1016, 882, 798, 768, 675$ cm^{-1}. UV/Vis (n-hexane, RT): $\lambda_{max,abs} = 509$ nm, $\lambda_{max,em} = 513$ nm, $\Phi = 77\%$; HRMS (MALDI$^+$) m/z: $[M]^{·+}$: calcd. for $[C_{44}H_{52}N_2Si_2]^{·+}$: 664.3664; found 664.3660; correct isotope distribution.

8,17-Bis{[tri*iso*propyl)silyl]ethynyl}naphtho[1,8-*bc*:5,4-*b′c′*]diacridine (6b): $R_f = 0.55$ (SiO$_2$; petroleum ether/dichloromethane 2:1, v/v); M.p.: ≥350 °C (decomposition); ^{1}H NMR ([D$_2$]-1,1,2,2-tetrachloro-ethane, 600 MHz, 70 °C): $\delta = 9.96$ (d, $J = 9.32$ Hz, 2H), 9.74 (s, 2H), 9.07 (d, $J = 9.32$ Hz, 2H), 8.55 (d, $J = 8.68$ Hz, 2H), 8.15 (d, $J = 8.33$ Hz, 2H), 7.93–7.97 (m, 2H), 7.67–7.71 (m, 2H), 1.42–1.49 ppm (m, 42H); ^{13}C{^{1}H} NMR (1,1,2,2-tetrachloroethane-d$_2$, 151 MHz, 70 °C): $\delta = 148.4, 142.5, 135.1, 132.7, 130.4, 129.7, 129.1, 128.2, 127.5, 126.7, 126.1, 125.6, 125.3, 123.4, 120.1, 105.9, 103.4, 18.8, 11.5$ ppm; IR (ATR): $\tilde{\nu} = 2940, 2863, 1461, 1068, 992, 881, 814, 785, 743, 676, 639, 595$ cm^{-1}; UV/Vis (n-hexane, RT): $\lambda_{max,abs} = 628$ nm, $\lambda_{max,em} = 634$ nm,
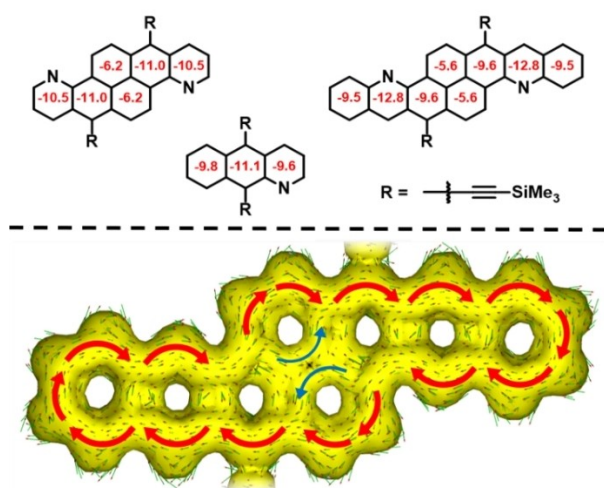

Figure 4. Top: NICS(1) values for **6a**, **6b** and **8**. Bottom: AICD plot[29] of compound **6b** (Gaussian 16: geometry optimization: B3LYP/def2-SVP// B3LYP/def2-TZVP; NICS calculations: GIAO-method B3LYP/def2-TZVP; TMS groups were used instead of TIPS;[23] AICD calculations: CSGT-method B3LYP/ def2-TZVP IO(10/93=1); the red arrows indicate the ring current flow magnetic field, the magnetic field vector is oriented out of plane; full AICD plots for **6a**, **6b** and **8** are given in the Supporting Information).

$\Phi = 35\%$; HRMS (MALDI$^+$) m/z: $[M+H]^+$: calcd. for $[C_{52}H_{57}N_2Si_2]^+$: 765.4055; found 765.4039; correct isotope distribution.

Supporting Information

Synthetic details, NMR spectra (^{1}H and ^{13}C), UV/Vis spectra, crystallographic data, cyclic voltammograms and FMOs as well as AICD plots of computationally studied molecules are given in the Supporting Information.

Acknowledgements

Conflict of Interest

The authors declare no conflict of interest.

[1] a) J. E. Anthony, *Chem. Rev.* **2006**, *106*, 5028–5048; b) J. E. Anthony, *Angew. Chem. Int. Ed.* **2008**, *47*, 452–483; *Angew. Chem.* **2008**, *120*, 460–492.

[2] H. Klauk, M. Halik, U. Zschieschang, G. Schmid, W. Radlik, W. Weber, *J. Appl. Phys.* **2002**, *92*, 5259–5263.

[3] C. Wang, B. Hu, J. Wang, J. Gao, G. Li, W.-W. Xiong, B. Zou, M. Suzuki, N. Aratani, H. Yamada, F. Huo, P. S. Lee, Q. Zhang, *Chem. Asian J.* **2015**, *10*, 116–119.

[4] a) D. N. Congreve, J. Lee, N. J. Thompson, E. Hontz, S. R. Yost, P. D. Reusswig, M. E. Bahlke, S. Reineke, T. Van Voorhis, M. A. Baldo, *Science* **2013**, *340*, 334–337; b) M. Einzinger, T. Wu, J. F. Kompalla, H. L. Smith, C. F. Perkinson, L. Nienhaus, S. Wieghold, D. N. Congreve, A. Kahn, M. G. Bawendi, M. A. Baldo, *Nature* **2019**, *571*, 90–94.

[5] a) C. S. Foote, *Acc. Chem. Res.* **1968**, *1*, 104–110; b) A. Greer, *Acc. Chem. Res.* **2006**, *39*, 797–804.

[6] M. Müller, L. Ahrens, V. Brosius, J. Freudenberg, U. H. F. Bunz, *J. Mater. Chem. C* **2019**, *7*, 14011–14034.

[7] a) J. E. Anthony, J. S. Brooks, D. L. Eaton, S. R. Parkin, *J. Am. Chem. Soc.* **2001**, *123*, 9482–9483; b) M. M. Payne, S. R. Parkin, J. E. Anthony, *J. Am. Chem. Soc.* **2005**, *127*, 8028–8029.

[8] W. Fudickar, T. Linker, *J. Am. Chem. Soc.* **2012**, *134*, 15071–15082.

[9] L. Ahrens, O. Tverskoy, S. Weigold, M. Ganschow, F. Rominger, J. Freudenberg, U. H. F. Bunz, *Angew. Chem. Int. Ed.* **2021**, *60*, 9270–9273; *Angew. Chem.* **2021**, *133*, 9356–9359.

[10] a) M. Müller, E. Rüdiger, S. Koser, O. Tverskoy, F. Rominger, F. Hinkel, J. Freudenberg, U. H. F. Bunz, *Chem. Eur. J.* **2018**, *24*, 8087–8091; b) M. Müller, S. Maier, O. Tverskoy, F. Rominger, J. Freudenberg, U. H. F. Bunz, *Angew. Chem. Int. Ed.* **2020**, *59*, 1966–1969; *Angew. Chem.* **2020**, *132*, 1982–1985.

[11] L. Zhang, A. Fonari, Y. Liu, A.-L. M. Hoyt, H. Lee, D. Granger, S. Parkin, T. P. Russell, J. E. Anthony, J.-L. Brédas, V. Coropceanu, A. L. Briseno, *J. Am. Chem. Soc.* **2014**, *136*, 9248–9251.

[12] Z. Wang, R. Li, Y. Chen, Y.-Z. Tan, Z. Tu, X. J. Gao, H. Dong, Y. Yi, Y. Zhang, W. Hu, K. Müllen, L. Chen, *J. Mater. Chem. C* **2017**, *5*, 1308–1312.

[13] L. Zhang, Y. Cao, N. S. Colella, Y. Liang, J.-L. Brédas, K. N. Houk, A. L. Briseno, *Acc. Chem. Res.* **2015**, *48*, 500–509.

[14] a) Y. Cao, Y. Liang, L. Zhang, S. Osuna, A.-L. M. Hoyt, A. L. Briseno, K. N. Houk, *J. Am. Chem. Soc.* **2014**, *136*, 10743–10751; b) S. Thomas, J. Ly, L. Zhang, A. L. Briseno, J.-L. Brédas, *Chem. Mater.* **2016**, *28*, 8504–8512.

[15] L. A. Stevens, K. P. Goetz, A. Fonari, Y. Shu, R. M. Williamson, J.-L. Brédas, V. Coropceanu, O. D. Jurchescu, G. E. Collis, *Chem. Mater.* **2015**, *27*, 112–118.

[16] M. L. Tang, A. D. Reichardt, P. Wie, Z. Bao, *J. Am. Chem. Soc.* **2009**, *131*, 5264–5273.

[17] J. Li, Q. Zhang, *ACS Appl. Mater. Interfaces* **2015**, *7*, 28049–28062.

[18] a) U. H. F. Bunz, *Chem. Eur. J.* **2009**, *15*, 6780–6789; b) J. Freudenberg, U. H. F. Bunz, *Acc. Chem. Res.* **2019**, *52*, 1575–1587; c) Q. Miao, *Synlett* **2012**, 326–336; d) Q. Miao, *Adv. Mater.* **2014**, *26*, 5541–5549.

[19] G. J. Richards, J. P. Hill, T. Mori K Ariga, *Org. Biomol. Chem.* **2011**, *9*, 5005–5017.

[20] L. Zhang, A. Fonari, Y. Zhang, G. Zhao, V. Coropceanu, W. Hu, S. Parkin, J. -L Brédas, A. L. Briseno, *Chem. Eur. J.* **2013**, *19*, 17907–17916.

[21] L. Ahrens, S. Hahn, F. Rominger, J. Freudenberg, U. H. F. Bunz, *Chem. Eur. J.* **2019**, *25*, 14522–14526.

[22] K. T. Potts, D. Bhattacharjee, E. B. Walsh, *J. Org. Chem.* **1986**, *51*, 2011–2021.

[23] *Gaussian 16, Revision C.01*, M. J. Frisch, G. W. Trucks, H. B. Schlegel, G. E. Scuseria, M. A. Robb, J. R. Cheeseman, G. Scalmani, V. Barone, G. A. Petersson, H. Nakatsuji, X. Li, M. Caricato, A. V. Marenich, J. Bloino, B. G. Janesko, R. Gomperts, B. Mennucci, H. P. Hratchian, J. V. Ortiz, A. F. Izmaylov, J. L. Sonnenberg, D. Williams-Young, F. Ding, F. Lipparini, F. Egidi, J. Goings, B. Peng, A. Petrone, T. Henderson, D. Ranasinghe, V. G. Zakrzewski, J. Gao, N. Rega, G. Zheng, W. Liang, M. Hada, M. Ehara, K. Toyota, R. Fukuda, J. Hasegawa, M. Ishida, T. Nakajima, Y. Honda, O. Kitao, H. Nakai, T. Vreven, K. Throssell, J. A. Montgomery, Jr., J. E. Peralta, F. Ogliaro, M. J. Bearpark, J. J. Heyd, E. N. Brothers, K. N. Kudin, V. N. Staroverov, T. A. Keith, R. Kobayashi, J. Normand, K. Raghavachari, A. P. Rendell, J. C. Burant, S. S. Iyengar, J. Tomasi, M. Cossi, J. M. Millam, M. Klene, C. Adamo, R. Cammi, J. W. Ochterski, R. L. Martin, K. Morokuma, O. Farkas, J. B. Foresman, D. J. Fox, Gaussian, Inc., Wallingford CT, **2016**.

[24] J. Thusek, M. Hoffmann, O. Hübner, S. Germer, H. Hoffmann, J. Freudenberg, U. H. F. Bunz, A. Dreuw, H.-J. Himmel, *Chem. Eur. J.* **2021**, *27*, 2072–2081.

[25] C. M. Cardona, W. Li, A. E. Kaifer, D. Stockdale, G. C. Bazan, *Adv. Mater.* **2011**, *23*, 2367–2371.

[26] A. Moliterni, D. Altamura, R. Lassandro, V. Olieric, G. Ferri, F. Cardarelli, A. Camposeo, D. Pisignano, J. E. Anthony, C. Giannini, *Acta Cryst.* **2020**, *B76*, 427–435.

[27] A. Camerman, J. Trotter, *Acta Crystallogr.* **1965**, *18*, 636–643.

[28] L. Pithan, D. Nabok, C. Cocchi, P. Beyer, G. Duva, J. Simbrunner, J. Rawle, C. Nicklin, P. Schäfer, C. Draxl, F. Schreiber, S. Kowarik, *J. Chem. Phys.* **2018**, *149*, 144701.

[29] a) D. Geuenich, R. Herges, *J. Phys. Chem. A* **2001**, *105*, 3214–3220; b) D. Geuenich, K. Hess, F. Koehler, R. Herges, *Chem. Rev.* **2005**, *105*, 3758–3772.

[30] M. Más-Montoya, R. P. Ortiz, D. Curiel, A. Espinosa, M. Allain, A. Facchetti, T. J. Marks, *J. Mater. Chem. C* **2013**, *1*, 1959–1969.

[31] a) D. Wang, Y. Wang, J. Zhao, L. Li, L. Miao, D. Wang, H. Sun, P. Yu, *Tetrahedron* **2016**, *72*, 5762–5768; b) N. Boudet, J. R. Lachs, P. Knochel, *Org. Lett.* **2007**, *9*, 5525–5528.

[32] J. Yamamoto, K. Kinpara, Y. Fukuda, Y. Nakasato, K. Uchida, T. Nishikawa, (Kyowa Hakko Kirin Co., Ltd.), **2011**, WO 2011093365.